

A glia-derived acetylcholine-binding protein that modulates synaptic transmission

August B. Smit*, Naweed I. Syed†, Dick Schaap‡§, Jan van Minnen*, Judith Klumperman||, Karel S. Kits*, Hans Lodder*, Roel C. van der Schors*, René van Elk*, Bertram Sorgedraeger*, Katjuša Brejc¶, Titia K. Sixma¶ & Wijnand P. M. Geraerts*

* Department of Molecular and Cellular Neurobiology, Research Institute Neurosciences Vrije Universiteit, Faculty of Biology, De Boelelaan 1087, 1081 HV Amsterdam, The Netherlands

¶ Division of Molecular Carcinogenesis, Netherlands Cancer Institute, Plesmanlaan 121, 1066 CX Amsterdam, The Netherlands

† Department of Cell Biology and Anatomy, University of Calgary, T2N4N1, Calgary, Canada

|| Department of Cell Biology, University Medical Center, Institute of Biomembranes and Center for Biogenetics, Heidelberglaan 100, 3584 CX Utrecht, The Netherlands

‡ Organon Teknika B.V., Bioscience Research Unit, Boseind 15, Boxtel, The Netherlands

There is accumulating evidence that glial cells actively modulate neuronal synaptic transmission. We identified a glia-derived soluble acetylcholine-binding protein (AChBP), which is a naturally occurring analogue of the ligand-binding domains of the nicotinic acetylcholine receptors (nAChRs). Like the nAChRs, it assembles into a homopentamer with ligand-binding characteristics that are typical for a nicotinic receptor; unlike the nAChRs, however, it lacks the domains to form a transmembrane ion channel. Presynaptic release of acetylcholine induces the secretion of AChBP through the glial secretory pathway. We describe a molecular and cellular mechanism by which glial cells release AChBP in the synaptic cleft, and propose a model for how they actively regulate cholinergic transmission between neurons in the central nervous system.

Chemical synaptic transmission is an important mode of signalling in the nervous system. The prevailing view is that chemical synaptic transmission exclusively involves bipartite synapses consisting of pre- and postsynaptic elements and a synaptic cleft, in which presynaptically released transmitter binds to cognate receptors in the postsynaptic cell. However, there is accumulating evidence that synapses have a more complex organization, and that glial cells not only actively participate in but can also modulate synaptic transmission^{1,2}.

For example, several studies have shown that presynaptically released glutamate not only binds receptors on the postsynaptic neuron^{3,4}, but may also activate AMPA (α -amino-3-hydroxy-5-methyl-4-isoxazole propionic acid)-type glutamate receptors on perisynaptic astrocytes^{5–9}, causing a rapid increase in intracellular Ca^{2+} concentration¹⁰ and Ca^{2+} -dependent release of glutamate from glia^{5,9,11,12}. Glutamate released by the perisynaptic astrocytes in turn activates NMDA (*N*-methyl-D-aspartate)-type receptors on the presynaptic neuron, thereby increasing the release of glutamate and enhancing synaptic transmission^{5,13,14}. Similar modulatory mechanisms involving perisynaptic glial cells have been suggested for GABA (γ -aminobutyric acid)-mediated synapses, where GABA released by astrocytes potentiates inhibitory synaptic transmission¹⁵, and for the cholinergic neuromuscular junction, where acetylcholine (ACh) released by activated perisynaptic glia^{16,17} probably feeds back onto the presynaptic nerve terminal¹⁸. Thus, for various types of synapse the glial cells complete a tripartite configuration, in which they can feed back modulatory signals to neuronal synaptic elements by releasing endogenous transmitter. As such, glial and neuronal cells can form integral modulatory components of synaptic function¹⁹.

In this study we explored the existence of alternative modulatory mechanisms, in which glial cells at tripartite synapses would interact directly with synaptic transmitters. We found that perisynaptic glial

cells of a molluscan cholinergic synapse respond to ACh by releasing a soluble ACh-receptor-like protein²⁰ into the synaptic cleft. This protein captures presynaptically released ACh and suppresses synaptic transmission. The release of this decoy glial receptor protein into the synaptic cleft provides a novel mechanism by which glial cells can modulate the efficacy of neuronal transmission in the central nervous system (CNS).

Glia modulate cholinergic synaptic transmission

To study the modulatory role of glia in interneuronal synaptic transmission, we cultured identified neurons from the CNS of the mollusc *Lymnaea stagnalis* with or without glial cells. Synapses between a presynaptic cholinergic neuron and its postsynaptic partner, and between a presynaptic dopaminergic neuron and its postsynaptic target, were reconstructed^{21–23}. Glial cells isolated from the CNS and plated close to the synapses migrated to the synapse within an hour. In the absence of glial cells, a train of induced action potentials in the cholinergic presynaptic neuron produced facilitatory excitatory postsynaptic potentials (EPSPs) in the postsynaptic cell, which often led to spiking activity (Fig. 1a). In the presence of glial cells, however, the presynaptically induced action potentials failed to elicit facilitatory EPSPs and action potentials in the postsynaptic cell (Fig. 1b). The glial cells did not affect dopaminergic synaptic transmission (Fig. 1c, d). These data show specific modulation by glial cells of the efficacy of cholinergic synaptic transmission, which is apparent only after high-frequency stimulation of the presynaptic cell. When neurons were cultured in a triplet configuration in which the presynaptic neuron forms two synapses with postsynaptic partners, only the synapse co-cultured with glia showed synaptic depression (Fig. 1f), leaving the non-glia-bearing synapse unaffected (Fig. 1e). Thus, the presence of glial cells at one synaptic site does not render the transmitter release machinery ineffective at other synapses.

To test the glial cell's ability to sense presynaptic transmitter release, we placed an isolated glial cell close to the presynaptic cholinergic neuron (Fig. 2a). Depolarization-induced transmitter

§ Present address: Intervet, de Körverstraat 35, 5830 AA Boxmeer, The Netherlands.

release from the presynaptic neuron was detected in the glial cell as non-synaptic depolarizing potentials. To define the transmitter-induced response in the glial cell in more detail, we recorded responses from an isolated glial cell to exogenously applied ACh under whole-cell voltage clamp conditions. Pressure application of 10 μ M ACh onto glial cells evoked a rapid inward current (Fig. 2b) with a median effective concentration (EC_{50}) of 2.4 μ M (Fig. 2d). These effects were mimicked by nicotine, but the nicotine-induced current inactivated much faster than the ACh-induced current (Fig. 2c). To define the nature of the receptor subtype that mediates the glial cholinergic response, we tested the effect of α -bungarotoxin (α -Bgt, a specific blocker of nAChRs of the vertebrate neuromuscular junction and of the homopentameric $\alpha 7$ -type nAChR²⁴). In the presence of α -Bgt the ACh-induced inward current was almost completely suppressed (Fig. 2e), indicating that the cholinergic

response in the glial cells may be mediated by an ionotropic, α -Bgt-sensitive nAChR. This glial nAChR has a reversal potential of 0 mV and conducts sodium ions, and is different from the chloride channels reported previously in molluscan neurons^{25,26}.

The physiological data led us to hypothesize that glial-cell-induced suppression of cholinergic synaptic transmission involves release of ACh from the presynaptic neuron, which depolarizes the glial cell through activation of an α -Bgt sensitive nAChR. The ACh-induced depolarization might in turn cause the release of an unknown factor, which suppresses synaptic transmission.

Glial cells express an nAChR-like protein

To test the above hypothesis, we first used rhodamine-conjugated α -Bgt to determine whether the $\alpha 7$ -type of nAChR was present on the glial cells. The α -Bgt labelling in sections of the *Lymnaea* CNS was intense, and in particular localized to glial cells (see below). Glial cells stained in culture showed a small amount of labelling of the cell surface (not shown); however, after permeabilization almost all labelling was punctate and localized to the cytoplasm of the glial cells (Fig. 3a). As the labelled unknown cytoplasmic factor probably contained an acetylcholine-binding site, we reasoned that it might be involved in the modulation of cholinergic transmission. To identify this factor, we used α -Bgt-biotin conjugated to streptavidin to

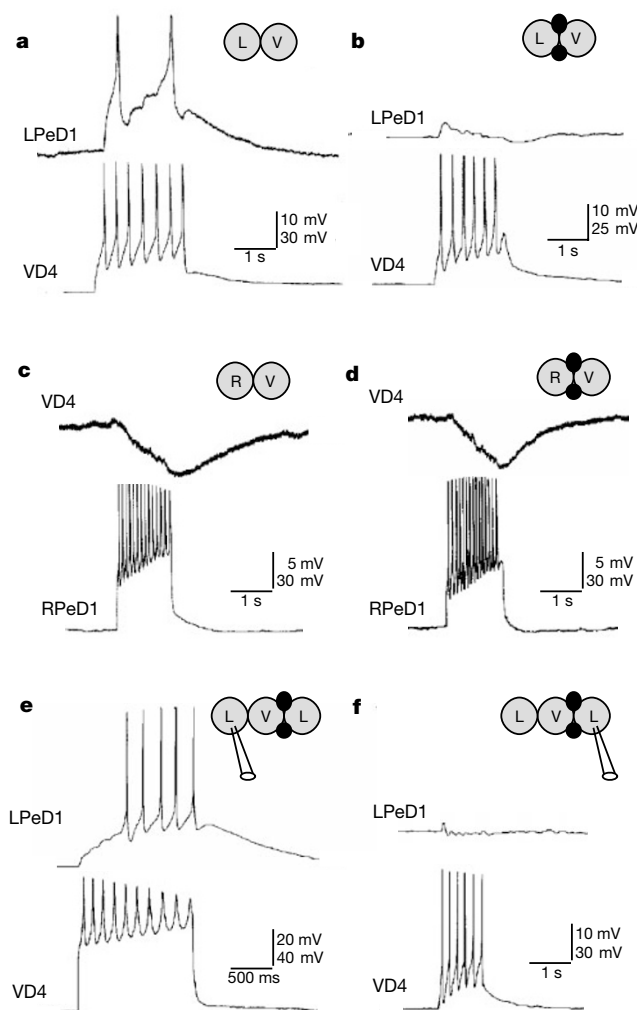


Figure 1 Glial cells cultured with synaptically paired neurons specifically inhibit cholinergic synaptic transmission. Synapse pairs represented schematically (V, VD4; L, LPeD1; R, RPeD1). Black circles, glia. **a**, VD4–LPeD1 pairs form a cholinergic excitatory synapse. Action potentials induced in the presynaptic cholinergic neuron VD4 generate EPSPs and action potentials in LPeD1 ($n = 13$ cell pairs). **b**, As in **a**, but cultured with glial cells that suppress synaptic transmission ($n = 13$). Residual response can be blocked by hexamethonium and is mediated by a nAChR. **c**, RPeD1–VD4 pairs form an inhibitory dopaminergic synapse. **d**, Co-cultured glia do not suppress dopaminergic synaptic inhibition. **e, f**, Dual-synapse configuration (two cholinergic synapses on a single presynaptic cell). **e**, In the synapse without co-cultured glia, VD4 action potentials lead to normal synaptic transmission with EPSPs and action potentials in LPeD1 ($n = 5$). **f**, In the synapse with co-cultured glia, synaptic transmission is suppressed ($n = 7$).

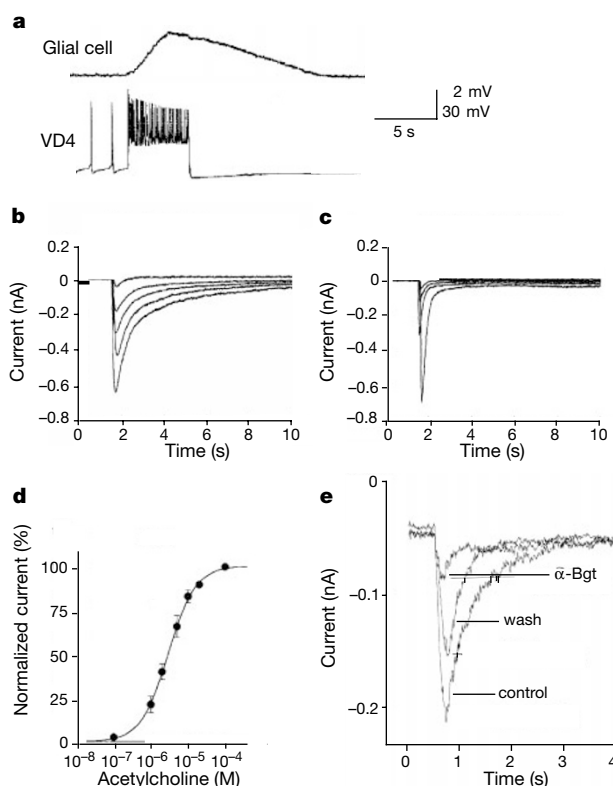


Figure 2 Glial cells detect ACh through a nicotinic ACh receptor. **a**, Glial cells held close to a VD4 neuron respond to action-potential-induced transmitter release with a compound depolarizing potential ($n = 5$). **b**, Whole-cell voltage clamp responses from an isolated glial cell to 10 μ M ACh applied by pressure ejection, recorded at holding potentials ranging from -100 mV (largest response) to -20 mV (smallest response; step size 20 mV). **c**, As in **b**, but showing responses to nicotine. **d**, Dose–response curve of glial cells to ACh (applied by pressure ejection). Responses were normalized to the maximum amplitude in the ACh experiment. Hill coefficient, 1.94. EC_{50} from fitted line is 2.4 μ M. Recorded at a holding potential of -80 mV; $n = 5$ cells; intervals between applications 50 s, sufficient to allow complete recovery from desensitization. **e**, Block of the current response to ACh (applied iontophoretically) by α -Bgt (10 μ M, applied by pressure ejection). Holding potential, -80 mV.

specifically pull down α -Bgt-binding proteins in particulate and soluble fractions of homogenates of the *Lymnaea* CNS. In contrast to subunits of nAChRs, which typically have relative molecular masses above 50,000 ($M_r > 50K$), SDS-polyacrylamide gel electrophoresis revealed a protein with an M_r of only around 25K, specifically enriched in the soluble fraction of the CNS homogenate (Fig. 3b). A partial amino-terminal amino-acid sequence, LDRA-DILYNIRQ, was obtained by western blotting and Edman degradation. On the basis of this, we generated a polymerase chain reaction (PCR) product on a complementary DNA library of the *Lymnaea* CNS and used it to screen the library. Sequence analysis of a 980-base-pair (bp) cDNA revealed a single open reading frame encoding a protein of 229 amino acids (Fig. 3c). The length of this cDNA corresponds well to the roughly 1,000-nucleotide transcript determined by northern blotting (Fig. 3d).

Because the α -Bgt-binding protein isolated from the CNS starts with Leu at position 20, the mature protein is only 210 amino acids long. In the precursor it is preceded by a signal sequence of 19 amino acids. To determine its relative molecular mass, the protein pulled down by α -Bgt was purified by high-performance liquid chromatography (HPLC), coupled on-line to a mass spectrometer (Q-TOF (quadrupole time-of-flight)) and shown to consist of a single molecular species of M_r 24,720.4 (not shown). Deglycosylation yields a protein with an M_r of only $23,832.9 \pm 2.8$ (not shown), corresponding to the mass of the mature protein predicted from the cDNA of 23,834. Thus, the α -Bgt-binding protein is a $\sim 23.8K$ glycoprotein with a glycosyl group of $M_r \sim 888$.

The α -Bgt-binding protein has moderate sequence identity with subunits of the Cys-loop family of ligand-gated ion channels (the nicotinic acetylcholine receptors (nAChRs), GABA_A, GABA_C, glycine and 5HT₃ receptors^{27–32}). These receptors comprise five

subunits, each consisting of an N-terminal extracellular domain, which is involved in ligand-binding, and a carboxy-terminal half containing four transmembrane segments (M1–M4), which make up the channel pore. The α -Bgt-binding protein is much shorter than these subunits and aligns only with the extracellular part, lacking pore-forming transmembrane regions. No homologous proteins of this size were found in sequence databases.

The highest sequence identity of AChBP is with the extracellular domains of the α -subunits of the nAChRs (Fig. 3c), and notably also with the $\alpha 7$ nAChR (23.9% in 210 amino acids). We therefore tentatively designated the α -Bgt-binding protein as acetylcholine-binding protein (AChBP). Although the sequence of AChBP is clearly related to those of the nAChRs, it is not a truncated form of a nAChR α -subunit. First, the AChBP transcript, at 1,050 bases, is too small to accommodate a full-length α -subunit of a *Lymnaea* nAChR (typically more than 1,800 nucleotides). We did not find alternatively spliced transcripts encoding a sequence-related nAChR. Second, rescreening the CNS library (at low stringency) using AChBP cDNA did not reveal any nAChR-related cDNAs among 50 sequenced. Third, as shown by affinity isolation and mass determination, the AChBP of 23.8K as predicted from the cDNA is present in the CNS. In addition, immunoprecipitation using an AChBP-specific antibody did not indicate the existence of larger proteins with AChBP epitopes.

In the nAChRs, both α - and non- α -subunits (or only α -subunits in the case of the $\alpha 7$ nAChR) contribute to ligand binding³², with the α -subunit contributing the principal components of the binding site. In the nAChR, specific residues residing in three loops are involved in ACh binding (for example, Trp 86, Tyr 93, Trp 149, Tyr 151, Tyr 190, the Cys 192, 193 doublet and Tyr 198 (ref. 32)). Except for Tyr 151, these residues are all conserved in AChBP

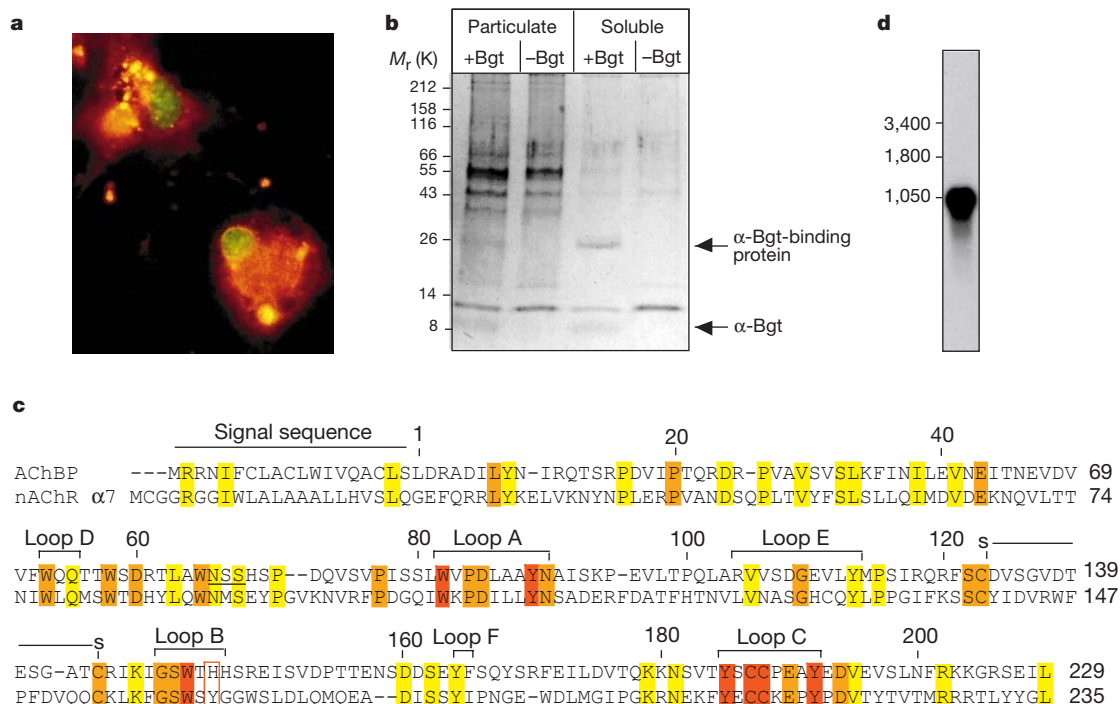


Figure 3 Characterization of α -bungarotoxin-binding protein from the *Lymnaea* CNS. **a**, α -Bgt-rhodamine labelling of glial cells freshly isolated from the CNS and after permeabilization. Cytoplasmic α -Bgt-rhodamine labelling is yellow/orange; nuclei counterstained with Syto-16 (green). **b**, Affinity isolation of α -Bgt-binding proteins from particulate and soluble fractions of 40 *Lymnaea* CNSs, with or without α -Bgt and run on 8% SDS-PAGE. An abundantly isolated 25K α -Bgt binding protein is indicated. **c**, Amino acid sequence of AChBP and comparison with ligand-binding subunit of the $\alpha 7$ nAChR.

Three ligand-binding loops A, B and C (as described for the nAChRs), and loops D, E and F of the complementary binding site, are indicated. Red, residues previously shown to be involved in ligand binding; orange, residues conserved in the nAChR family; yellow, residues conserved between AChBP and $\alpha 7$ nAChR. Underlined, consensus glycosylation site. **d**, Northern blotting at low stringency indicates the existence of a single AChBP transcript (numbers indicate bases).

(Fig. 3c). The characteristically conserved cysteine disulphide bridge forming a 15-residue loop in the extracellular domain of the ligand-binding subunits of nAChRs is present at position 123–136 in AChBP (Fig. 3c). However, the cysteines are spaced by only 12 instead of 13 amino acids, and sequence conservation of the loop residues is lost. The sequence similarity between AChBP and the nAChR α -subunits, and in particular the conservation of the ligand-binding residues, led us to test the ligand-binding characteristics of AChBP with nAChR ligands.

Multimerization and ligand binding by AChBP

To test ligand binding by AChBP, we expressed the protein in yeast²⁰ (recAChBP). When tested under native conditions on a gel-permeation column it runs at an apparent M_r of ~160K (Fig. 4a), indicating that it forms a (soluble) multimer of 5 or 6 subunits (X-ray crystallography²⁰ showed that AChBP was a pentamer). Subunits of the nAChRs form homo- and heteropentamers, both *in vivo* and *in vitro*^{33,34}. In the $\alpha 7$ nAChR the determinants for pentamerization have been mapped to regions in both the extracellular domain³⁵ and the first transmembrane domain³⁶. In AChBP, which is analogous to the extracellular domain of nAChRs, this domain is apparently sufficient to determine pentamerization. Studies on the $\alpha 7$ nAChR have indicated the importance of the M1 region in the expression of the extracellular domain³⁷.

To determine the ligand-binding characteristics of the AChBP multimer, we performed a series of binding assays. First, we determined the binding curve of α -Bgt to recAChBP, and calculated an affinity of 3.5 nM (Fig. 4b). Using 125 I- α -Bgt in a competitive binding assay we then tested ligands of several types of ligand-gated ion channel on recAChBP (ACh, serotonin, GABA, glycine and

glutamate). Both ACh and serotonin competed with 125 I- α -Bgt binding at 4.2 μ M and 269 μ M, respectively, whereas GABA, glycine and glutamate did not (Fig. 4c). AChBP binds ACh but does not contain esterase activity (not shown). Second, we studied the ligand-binding characteristics of AChBP in more detail using agonists (Fig. 4d) and antagonists (Fig. 4e) of the AChRs. Nicotine, the typical agonist of nAChRs, is a high-affinity ligand of recAChBP (IC_{50} 98 nM). The apparent affinity of ACh for AChBP is 42-fold lower than that of nicotine, a typical feature of the $\alpha 7$ nAChR³⁸. In addition, the affinities for both ligands are much lower (ACh, 1,000-fold; nicotine, 18-fold) than observed for the high-affinity heteromeric nAChRs (for example, the $\alpha 4\beta 2$ subtype). Epibatidine, a high-affinity agonist of nAChRs³⁹, also binds with high affinity to recAChBP (IC_{50} 1.4 nM). Other cholinergic agonists bind with low affinity: for example, carbachol and choline have IC_{50} s of 43 and 190 μ M, respectively.

Typical antagonists of the nAChRs, such as tubocurarine and α -Bgt, have a high affinity for AChBP (IC_{50} s of 93 nM and 3.5 nM, respectively). The cholinergic antagonist succinylcholine has a very low affinity for AChBP (IC_{50} 7.9 mM). Muscarinic receptor antagonists also bind to recAChBP with relatively high affinities: for example, the muscarinic allosteric modulator gallamine (IC_{50} 39 nM) and the muscarinic antagonist atropine (IC_{50} 5.3 μ M). Finally, bipinnatin-B, a synthetic form of coral toxin and a general blocker of nAChRs⁴⁰, covalently blocked recAChBP (see Supplementary Information). The binding characteristics of recAChBP are summarized in Fig. 4f. In contrast to the $\alpha 7$ nAChR⁴¹ (Hill coefficient for ACh ~1.4), AChBP has Hill coefficients of less than 1 for all agonists and some antagonists, which might represent true negative cooperativity or some micro-heterogeneity due to

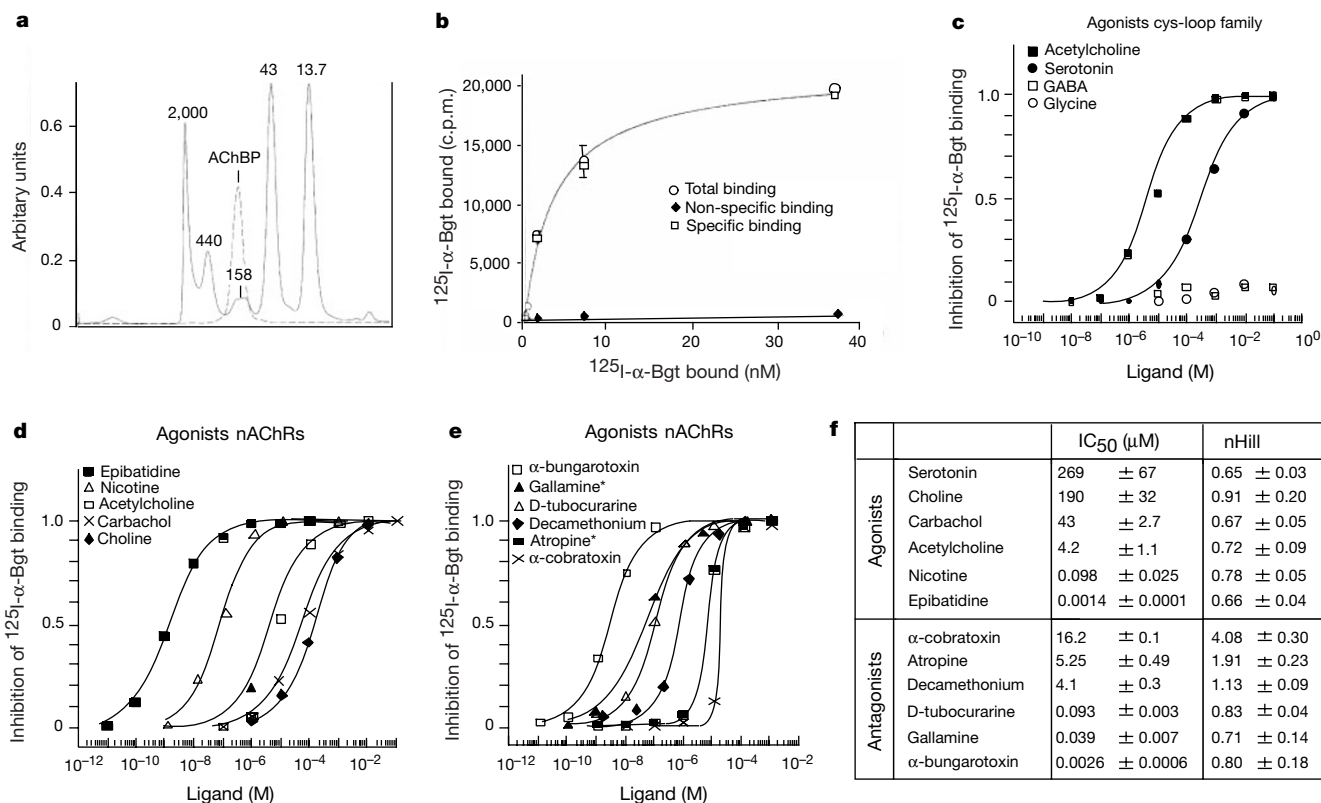


Figure 4 Ligand-binding characteristics of AChBP. **a**, The running profile of recAChBP under native conditions. Marker proteins and AChBP were run separately and chromatograms were superimposed. M_r as indicated. **b**, Saturation curve of 125 I- α -Bgt to AChBP. **c**, Various ligands, ACh, serotonin, glycine, GABA, and glutamate, were incubated with His-tagged AChBP and allowed to compete for binding with 125 I- α -Bgt. Binding

curves for ACh and serotonin and IC_{50} values are indicated. GABA, glycine, and glutamate do not show competition binding. **d**, **e**, Competition binding on AChBP as in **c** with agonists and antagonists of the nAChRs. **f**, Summary of IC_{50} values and Hill coefficients (nHill) of the plots in **c**–**e**. Note that gallamine and atropine have mixed pharmacology and are also antagonists of the muscarinic AChRs.

either non-equivalence of the subunits or slightly different forms of symmetric oligomers. Thus, AChBP shows a mixed nicotinic–muscarinic pharmacology with many features of nAChRs of the $\alpha 7$ - and $\alpha 9$ -subtypes^{42,43}.

Cellular and subcellular localization of AChBP

Localization studies of AChBP in the *Lymnaea* CNS, tested by labelling of CNS sections with rhodamine- α -Bgt, immunocytochemistry and *in situ* hybridization of AChBP, show co-expression of the AChBP gene and protein in glial cells (Fig. 5a–c). The AChBP-expressing glial cells are localized between neuronal cell bodies (Fig. 5d, e) and are also densely packed between axon terminals (Fig. 5c, g). When stained in culture, only about 50% of the glial cells produce AChBP.

To determine the cellular route for the secretion of AChBP in the glial cells, we performed immunogold labelling of AChBP on ultrathin cryosections of the *Lymnaea* CNS. AChBP protein was readily visualized in the early secretory pathway of the glial cells, for example in the endoplasmic reticulum and the Golgi apparatus (Fig. 5f). In addition, it was found in denser granule-like compartments that occurred near the Golgi apparatus (Fig. 5f) and in the long processes of the cells (Fig. 5g). The morphology, subcellular distribution and high content of AChBP in these dense granules

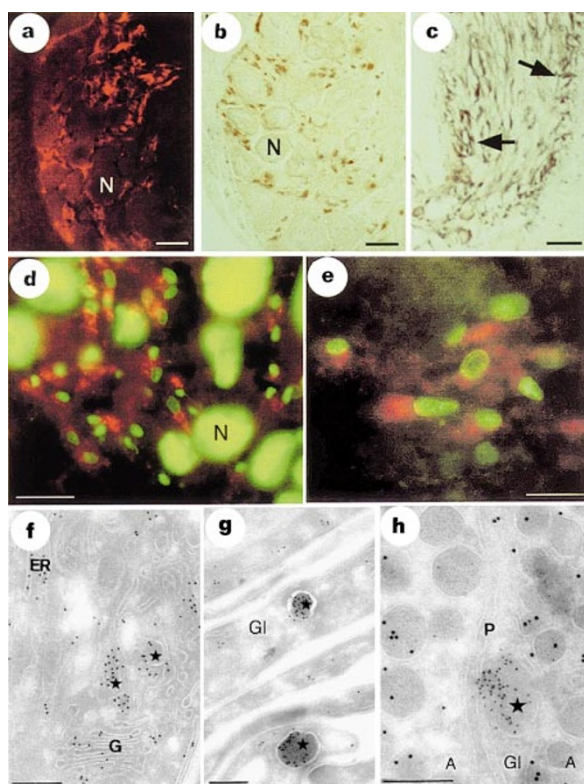


Figure 5 Cellular and subcellular expression of AChBP. **a**, Rhodamine- α -Bgt labelling of the cerebral commissure of the *Lymnaea* CNS, showing AChBP-containing glial cells. **b**, Immunostaining of glial cells in the cerebral ganglion. **c**, *In situ* hybridization showing glial cells between axon endings of egg-laying hormone neurons in cerebral commissure (arrows). Scale bar, 100 μ m; **N**, neuron. **d**, **e**, Rhodamine- α -Bgt labelling of glia (punctate labelling) in the cerebral ganglia. Neurons are devoid of signal. Scale bar, 100 μ m (**d**), 30 μ m (**e**). **f–h**, Ultrathin cryosections of the *Lymnaea* CNS, immunogold labelled for AChBP (10 nm gold) or double-labelled for AChBP (5 nm gold) and egg-laying hormone (10 nm gold). **f**, Anti-AChBP densely labels the endoplasmic reticulum (ER) and Golgi apparatus (G) of a glial cell. Stars, LDCVs in AChBP-containing glia. **g**, AChBP LDCVs in glial processes (Gl). **h**, A glial cell process (Gl) containing an LDCV with AChBP (star) between axons (A) of egg-laying hormone neurons, with hormone-containing vesicles. P, plasma membrane; bars in **f–h**, 200 nm.

indicate that they probably represent large, dense-core secretory vesicles (LDCVs) involved in AChBP secretion.

We then focused on neuroendocrine cells that produce the egg-laying hormone, because their electrical activity is known to be regulated by ACh. Double-immunolabelling for AChBP and a peptide of the egg-laying hormone precursor showed AChBP-containing LDCVs in glial cell processes that were intermingled with the axon terminals of cells producing egg-laying hormone (Fig. 5h).

Release of AChBP from glia is mediated by an nAChR

Because AChBP is produced in the secretory pathway of glial cells and binds acetylcholine, and because ACh depolarizes glial cells, we directly assessed whether ACh also induces the cellular release of AChBP. After metabolic labelling of glial cells *in vitro* with ³⁵S-labelled cysteine/methionine, we quantified the release of AChBP using immunoprecipitation (Fig. 6a). ACh (10 μ M) applied to glial cells *in vitro* induced AChBP release (Fig. 6b). The induction of AChBP release by ACh could be blocked almost completely by α -Bgt (Fig. 6b), which indicates that the glial nAChR is involved in the release of AChBP.

Suppression of cholinergic transmission by AChBP

Because the glial cells suppress cholinergic transmission, produce AChBP and release it in response to ACh, it is important to show that AChBP can suppress synaptic transmission. To test this, we reconstructed the cholinergic synapse *in vitro* and tested synaptic transmission in the absence (Fig. 7a) and presence (Fig. 7b) of recAChBP (10 μ M). We found that recAChBP significantly suppressed synaptic transmission, in a manner similar to that observed with co-cultured glial cells (Fig. 1b). The first EPSP was largely unperturbed, whereas subsequent synaptic potentials were completely or significantly suppressed by recAChBP. Bipinnatin-B-inactivated AChBP, on the other hand, failed to suppress synaptic transmission between the paired cells (Fig. 7c). In this set-up, bipinnatin-B left intact the response of the postsynaptic receptors (Fig. 7d). Finally, to test whether in the neuron–glia co-culture it is indeed endogenous AChBP that suppresses synaptic transmission, we used α -Bgt to block binding of ACh to AChBP and to stop the release of AChBP mediated by the glial nAChR. Consistent with our hypothesis, addition of α -Bgt to the culture removed the glial (AChBP)-induced suppression of synaptic transmission between the paired cells (Fig. 7e, f). Our data show that AChBP can capture presynaptically released ACh and thus act as a synaptic ACh buffer, causing immediate suppression of synaptic transmission.

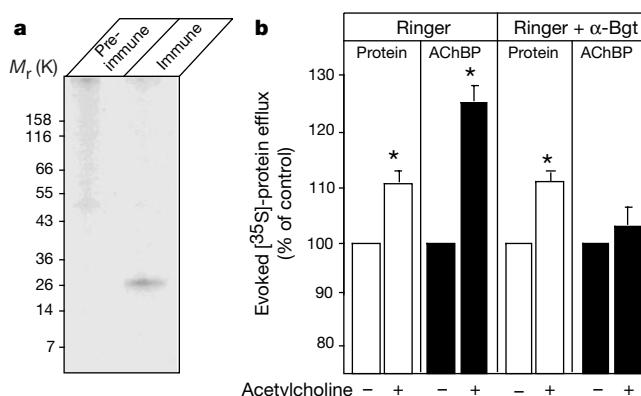


Figure 6 Glial cells release AChBP. **a**, Immunoprecipitation of radiolabelled AChBP from the *Lymnaea* CNS using a polyclonal antibody. **b**, Induced release of radiolabelled AChBP or other cellular proteins by ACh, quantified after (immuno)precipitation. Release of AChBP is almost completely blocked by pre-incubating glia in α -Bgt. Asterisk, significantly different from control ($P < 0.05$).

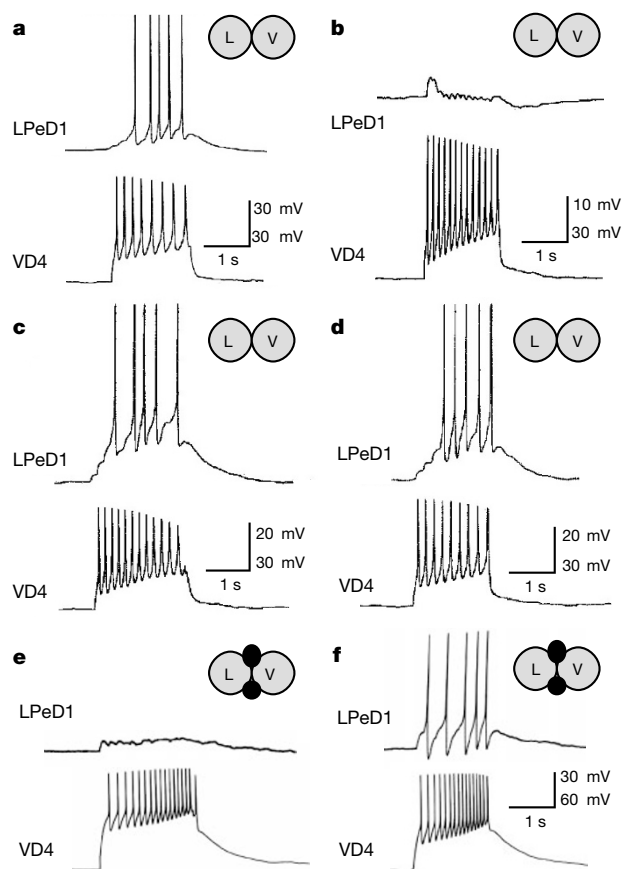


Figure 7 AChBP suppresses cholinergic neurotransmission. **a**, Normal cholinergic excitatory synaptic transmission between VD4 and LPeD1. **b**, Synaptic transmission is suppressed by superfusion with 10 μ M AChBP. **c**, Synaptic transmission is not suppressed by superfusion with biotinylated AChBP. **d**, Biotinylated AChBP superfusion alone does not suppress synaptic transmission. **e**, Suppression of transmission in the glia–neuron co-culture (VD4–LPeD1–glia) is lifted (**f**) by the addition of α -bungarotoxin. Symbols as in Fig. 1.

Discussion

Using a combined molecular, pharmacological and physiological approach we have identified a soluble transmitter receptor, AChBP, and shown that it suppresses cholinergic synaptic transmission. Its inclusion in the secretory pathway of glial cells and its stimulus-dependent release into the synaptic cleft constitute a novel molecular and cellular mechanism that is sufficient to account for its modulatory role in synaptic transmission.

On the basis of our *in vitro* data (Fig. 6), we suggest that there is a basal level of AChBP in the synaptic cleft, maintained by continuous release from the synaptic glial cells. Under conditions of active presynaptic transmitter release, high millimolar concentrations of free ACh⁴⁷ will probably activate both postsynaptic receptors and the nAChRs on the synaptic glial cells (EC_{50} in the micromolar range; Fig. 2d), which would enhance the release of AChBP, thus increasing its concentration in the synaptic cleft (Fig. 8). This may either diminish or terminate the ongoing ACh response, or raise the concentration of basal AChBP to the extent that subsequent responses to ACh are decreased. Accurate models of the kinetics of AChBP in synaptic modulation will require more data, such as concentrations of ACh, AChE and postsynaptic nAChRs, the localization and individual affinities of these components and the diffusion characteristics of ACh^{44–46}. Similarly, they will have to incorporate the effect of the ultrastructure of the synapse that

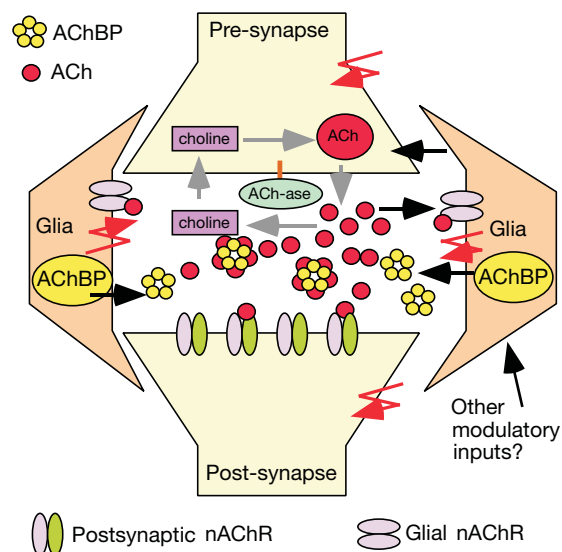


Figure 8 Model of the role of AChBP in neurotransmission. A basal level of AChBP is present in the synaptic cleft. Presynaptic ACh release can lead to activation of postsynaptic receptors and to EPSPs. In parallel, nAChRs on glia are activated, causing increased release of AChBP into the synapse, which leads to suppression of cholinergic transmission (see Discussion).

determines the kinetic properties of these constituents (that is, small processes of synapse-invaginating glial cells that locally release AChBP).

However, for the sake of simplicity one could consider two extreme scenarios of cholinergic transmission—under high and low concentrations of AChBP. On the basis of the measured dissociation constant of 4 μ M, a concentration of 80 μ M AChBP and 80 μ M ACh would generate a free ACh concentration of 16 μ M, which is probably sufficient to activate postsynaptic receptors. At high AChBP concentrations (for example, 400 μ M), however, the concentration of free ACh would drop to 0.9 μ M, which is likely to be insufficient to activate postsynaptic receptors. Moreover, the activation of postsynaptic nAChRs at concentrations below their EC_{50} value for ACh drops with the square of the ACh concentration⁴⁴, thus limiting further nAChR activation at low ACh concentrations. So, if AChBP release would bring down the free ACh concentration to values below the EC_{50} , the postsynaptic response would be substantially affected. As such, the concentration of AChBP in the synapse might critically determine whether transmission is fully active or suppressed.

When ACh is bound to AChBP in the synaptic cleft, acetylcholinesterase will hydrolyse only the free ACh, thereby keeping the ACh concentration minimal and draining it from the AChBP buffer. Under this condition, ACh bound to AChBP is unable to activate postsynaptic nAChRs, while the concentration of remaining free transmitter might not be sufficient to do so.

In our experimental set-up AChBP leads to complete, or nearly complete (Fig. 7e), suppression of synaptic transmission. *In vivo*, however, synaptic glial cells may be less numerous, exhibit different thresholds for AChBP release or even have different morphology in the synaptic cleft, hence leading to a less stringent AChBP block and a more balanced modulation of the efficacy of synaptic transmission. Moreover, *in vivo*, synaptic glial cells might integrate various signals and even at inactive synapses tune the rate of AChBP release (up or down), thereby setting the basal synaptic level of AChBP on which modulation of synaptic efficacy will occur during active transmission (Fig. 8). In addition to a regulated release of AChBP, its removal from the synaptic cleft might also be actively controlled to determine its precise concentration in the synaptic cleft. □

Methods

Cell culture

Ganglia were isolated and prepared for dissection⁴⁸. Identified neurons were isolated from the CNS, plated on poly-L-lysine-coated dishes containing brain-conditioned medium, and paired in a soma–soma configuration as described²¹. Glial cells were extracted from pedal ganglia using a glass pipette (30–40 µm diameter) and gentle pressure suction. Isolated glia were then gently flushed close to the soma–soma paired neurons. Identified neurons used^{21,22} were: VD4, visceral–dorsal 4 neuron; LPeD1, left pedal–dorsal 1 neuron; RPeD1, right pedal–dorsal 1 neuron.

Electrophysiology

For intracellular recordings, conventional sharp electrode recording techniques were used⁴⁸. Whole-cell voltage clamp recordings were made at room temperature from freshly dissociated glial cells in saline containing (in mM) 30 NaCl, 1.7 KCl, 10 NaH₂SO₄, 1.5 MgCl₂, 4 CaCl₂, 5 NaHCO₃ and 10 HEPES, pH 7.8, with NaOH, using an EPC7 amplifier (List) and pipettes filled with saline containing (in mM) 29 KCl, 2 MgATP, 2.3 CaCl₂, 11 EGTA, 10 HEPES, pH 7.4, with KOH. After reaching whole-cell configuration, cell capacitance was compensated (average 4.95 ± 0.97 pF); series resistance was not compensated. ACh, nicotine and α-Bgt were applied by pressure application.

Pharmacology

For competition experiments, we used 0.2 nM AChBP in assay buffer (PBS; Tris, 20 mM; BSA, 1 mg ml⁻¹; pH 8.0). Ligands or buffer were added and incubated for 15 min at 20 °C. The final concentration of [¹²⁵I]-α-Bgt was 0.1 nM. After incubation with continuous shaking for 1 h at 20 °C, we added Co²⁺ bead slurry (Clontech) pre-washed with assay buffer. After 15 min the beads were washed, centrifuged and scintillation counted. Experiments were performed fourfold. Curves were fitted to the data.

PCR and cDNA library screening

A degenerate oligonucleotide was synthesized on the basis of residues 1–10 of AChBP (LDRADILYNI), 5'-CGGATCCGA(TC)(AC)GIGC(GATC)GA(TC)AT(ATC)(TC)T(GATC)TA(TC)AA(TC)AT-3' and used for PCR in combination with a λZAPII vector primer. PCR: 45 cycles of 94 °C, 20 s; 53 °C, 30 s; and 72 °C, 1 min. Hybridization for λZAPII CNS cDNA library screening was performed in 6× SSC (1× SSC: 0.15 M NaCl and 0.015 M Na-citrate), 0.2% SDS, 5× Denhardt's and 10 µg ml⁻¹ herring sperm DNA at 65 °C for 18 h. Washing was in 0.2× SSC, 0.2% SDS at 65 °C for 30 min.

Gel filtration

To determine the relative molecular mass of the multimer, recAChBP (45 µg) dissolved in running buffer (20 mM Tris/HCl, pH 8.0, 150 mM NaCl, 0.02% Na-azide) was run on a Superdex 200 HiLoad 16/60 column (Pharmacia). Marker proteins were run separately in running buffer (50 mM Tris/HCl, pH 8.0, 150 mM NaCl, 3 mM β-mercaptoethanol) on the same column. Absorbance detection was at 254 nm.

In situ hybridization and cytochemistry

For *in situ* hybridization, digoxigenin-labelled run-off sense and antisense cRNAs to the coding region of AChBP were synthesized using T7 or T3 RNA polymerase and digoxigenin-UTP labelling (Boehringer). Signal was detected by using sheep anti-digoxigenin, conjugated to alkaline phosphatase. For immunolabelling, a mouse polyclonal antibody raised against recAChBP was used, and detected by a sheep anti-mouse antibody (Dako), conjugated to horseradish peroxidase⁴⁹. For α-Bgt labelling sections were incubated in 1:100 diluted rhodamine-α-Bgt (Molecular Probes) in PBS for 60 min, washed 3 × 5 min in PBS and viewed with a fluorescence microscope.

Immunogold labelling

All studies were performed on adult specimens of *Lymnaea*. Ultrathin cryosections were prepared and (double)-immunolabelled by the protein A gold technique⁵⁰. Primary antibodies were a mouse polyclonal anti-AChBP and an affinity-purified polyclonal antibody against the α-caudodorsal cell peptide (anti-ELH). Grids were analysed in a Philips EM3000 electron microscope.

Sequence and mass determination

We homogenized 80 *Lymnaea* CNSs in lysis buffer (PBS (16 mM Na₂HPO₄, 4 mM NaH₂PO₄, pH 7.4, 150 mM NaCl), 0.5% Nonidet P-40, 0.1% Triton, 0.2% Tween-20) containing protease inhibitors. No detergents were used in making a soluble fraction. Lysates were cleared by centrifugation at 12,000g for 5 min. Streptavidin-coated magnetic beads (Dyna; 5 mg) were saturated with α-Bgt-Biotin (Molecular Probes), washed in PBS, incubated with the cleared lysate for 1 h and washed in PBS. In control α-Bgt was omitted. Proteins bound to α-Bgt-beads were eluted in 10 µl PBS, 10⁻⁴ M nicotine for 1 h. The eluent was separated on a microcolumn LC system and electrospray mass spectra were acquired on a mass spectrometer (Micromass, Q-TOF). Sequence analysis of α-Bgt binding protein was by the same protocol, followed by SDS-PAGE, western blotting on PVDF and Edman degradation using a protein sequencer (Model 473A, ABI).

Immunoprecipitation

Five *Lymnaea* CNSs were desheathed and mass dissociated in a culture dish, allowing glial cells to adhere selectively. Glia were incubated in 5 ml HEPES buffered saline (HBS; 5 mM

HEPES (pH 7.9), 51 mM NaCl, 1.7 mM KCl, 4.1 mM CaCl₂, 1.5 mM MgCl₂) containing 20 µCi ml⁻¹ [³⁵S]-Met/Cys mixture (Tran-S, ICN) at room temperature for 4 h and rinsed with HBS. α-Bgt was used at 10⁻⁷ M for 10 min and ACh at 10⁻⁵ M for 5 min, all in HBS. AChBP antibody was added to the releasate, incubated at 16 °C for 2 h, and Protein-A agarose (Gibco) was added for 1 h. Beads were rinsed with HBS, resuspended in SDS sample buffer and boiled, and the precipitated radiolabelled AChBP was analysed in triplicate on 8% SDS-PAGE and quantified using densitometry.

Received 4 January; accepted 19 April 2001.

- Araque, A., Parpura, V., Sanzgiri, R. P. & Haydon, P. G. Tripartite synapses: glia the unacknowledged partner. *Trends Neurosci.* **22**, 208–215 (1999).
- Smith, S. J. Do astrocytes process neural information? *Prog. Brain Res.* **94**, 119–136 (1992).
- Dani, J. W., Chernjavsky, A. & Smith, S. J. Neuronal activity triggers calcium waves in hippocampal astrocyte networks. *Neuron* **8**, 429–440 (1992).
- Pasti, L., Pozzan, T. & Carmignoto, G. Long-lasting changes of calcium oscillations in astrocytes. A new form of glutamate-mediated plasticity. *J. Biol. Chem.* **270**, 15203–15210 (1995).
- Parpura, V. et al. Glutamate-mediated astrocyte–neuron signaling. *Nature* **369**, 744–747 (1994).
- Nedergaard, M. Direct signaling from astrocytes to neurons in cultures of mammalian brain cells. *Science* **263**, 1768–1771 (1994).
- Murphy, T. H., Blatter, L. A., Wier, W. G. & Baraban, J. M. Rapid communication between neurons and astrocytes in primary cortical cultures. *J. Neurosci.* **13**, 2672–2679 (1993).
- Newman, E. A. & Zahs, K. R. Modulation of neuronal activity by glial cells in the retina. *J. Neurosci.* **18**, 4022–4028 (1998).
- Pasti, L., Volterra, A., Pozzan, T. & Carmignoto, G. Intracellular calcium oscillations in astrocytes: a highly plastic, bidirectional form of communication between neurons and astrocytes in situ. *J. Neurosci.* **17**, 7817–7830 (1997).
- Cornell-Bell, A. H., Finkbeiner, S. M., Cooper, M. S. & Smith, S. J. Glutamate induces calcium waves in cultured astrocytes: long-range glial signaling. *Science* **247**, 470–473 (1990).
- Calegari, F. et al. A regulated secretory pathway in cultured hippocampal astrocytes. *J. Biol. Chem.* **274**, 22539–22547 (1999).
- Porter, J. T. & McCarthy, K. D. Hippocampal astrocytes in situ respond to glutamate released from synaptic terminals. *J. Neurosci.* **16**, 5073–5081 (1996).
- Araque, A., Parpura, V., Sanzgiri, R. P. & Haydon, P. G. Glutamate-dependent astrocyte modulation of synaptic transmission between cultured hippocampal neurons. *Eur. J. Neurosci.* **10**, 2129–2141 (1998).
- Araque, A., Sanzgiri, R. P., Parpura, V. & Haydon, P. G. Calcium elevation in astrocytes causes an NMDA receptor-dependent increase in the frequency of miniature synaptic currents in cultured hippocampal neurons. *J. Neurosci.* **18**, 6822–6829 (1998).
- Kang, J., Jiang, L., Goldman, S. A. & Nedergaard, M. Astrocyte-mediated potentiation of inhibitory synaptic transmission. *Nature Neurosci.* **1**, 683–692 (1998).
- Jahromi, B. S., Robitaille, R. & Charlton, M. P. Transmitter release increases intracellular calcium in perisynaptic Schwann cells in situ. *Neuron* **8**, 1069–1077 (1992).
- Robitaille, R., Jahromi, B. S. & Charlton, M. P. Muscarinic Ca responses resistant to muscarinic agonists at the perisynaptic Schwann cells at the frog neuromuscular junction. *J. Physiol.* **504**, 337–347 (1997).
- Robitaille, R. Modulation of synaptic efficacy and synaptic depression by glial cells at the frog neuromuscular junction. *Neuron* **21**, 847–855 (1998).
- Theodosis, D. T. & Poullain, D. A. Activity-dependent neuronal glial and synaptic plasticity in the adult mammalian hypothalamus. *Neurosci.* **57**, 501–535 (1993).
- Brej, K. et al. Crystal structure of an ACh-binding protein reveals the ligand-binding domain of nicotinic receptors. *Nature* **411**, 269–276 (2001).
- Feng, Z. P., Klumperman, J., Lukowiak, K. & Syed, N. I. In vitro synaptogenesis between the somata of identified *Lymnaea* neurons requires protein synthesis but not extrinsic growth factors or substrate adhesion molecules. *J. Neurosci.* **17**, 7839–7849 (1997).
- Hamakawa, T. et al. Excitatory synaptogenesis between identified *Lymnaea* neurons requires extrinsic trophic factors and is mediated by receptor tyrosine kinases. *J. Neurosci.* **19**, 9306–9312 (1999).
- Woodin, M. A., Hamakawa, T., Takasaki, K. & Syed, N. I. Trophic factor-induced plasticity of synaptic connections between identified *Lymnaea* neurons. *Learn. Mem.* **6**, 307–316 (1999).
- Orr-Urtreger, A. et al. Mice deficient in the α7 neuronal nicotinic acetylcholine receptor lack α7 bungarotoxin binding sites and hippocampal fast nicotinic currents. *J. Neurosci.* **17**, 9165–9171 (1997).
- Gardner, D. & Kandel, E. R. Interconnections of identified multiaction interneurons in buccal ganglia of *Aplysia*. *J. Neurophys.* **40**, 349–361 (1977).
- Yeoman, M. S., Parish, D. C. & Benjamin, P. R. A cholinergic modulatory interneuron in the feeding system of the snail, *Lymnaea*. *J. Neurosci.* **70**, 37–50 (1993).
- Le Novere, N. & Changeux, J. P. Molecular evolution of the nicotinic acetylcholine receptor: an example of multigene family in excitable cells. *J. Mol. Evol.* **40**, 155–172 (1995).
- Devillers-Thiery, A., Galzi, J. L., Eiselé, J. L., Bertrand, S. & Changeux, J. P. Functional architecture of the nicotinic acetylcholine receptor: a prototype of ligand-gated ion channels. *J. Membrane Biol.* **136**, 97–112 (1993).
- Karlin, A. & Akabas, M. H. Toward a structural basis for the function of nicotinic acetylcholine receptors and their cousins. *Neuron* **6**, 1231–1244 (1995).
- Mehta, A. K. & Ticku, M. K. An update on GABA_A receptors. *Brain Res. Rev.* **2–3**, 196–217 (1999).
- Betz, H. et al. Structure and functions of inhibitory and excitatory glycine receptors. *Annu. NY Acad. Sci.* **868**, 667–676 (1999).
- Corringer, P. J., Le Novere, N. & Changeux, J. P. Nicotinic receptors at the amino acid level. *Annu. Rev. Pharmacol. Toxicol.* **40**, 431–458 (2000).
- Drisdell, R. C. & Green, W. N. Neuronal α-Bungarotoxin receptors are α7 subunit homomers. *J. Neurosci.* **20**, 133–139 (2000).
- Green, W. N. Channel assembly: creating structures that function. *J. Gen. Physiol.* **113**, 163–169 (1999).
- Verall, S. & Hall, Z. W. The N-terminal domain of the acetylcholine receptor subunits contain recognition signals for the initial steps of receptor assembly. *Cell* **68**, 23–31 (1992).
- Wang, Z. Z., Hardy, S. F. & Hall, Z. W. Assembly of the nicotinic acetylcholine receptor. The first

- transmembrane domains of truncated alpha and delta subunits are required for heterodimer formation *in vivo*. *J. Biol. Chem.* **271**, 27575–27584 (1996).
37. Wells, G. B., Anand, R., Wang, F. & Lindstrom, J. Water-soluble nicotinic acetylcholine receptor formed by alpha7 subunit extracellular domains. *J. Biol. Chem.* **273**, 964–973 (1998).
38. Corringer, P. J. *et al.* Critical elements determining diversity in the agonist binding and desensitization of neuronal nicotinic acetylcholine receptors. *J. Neurosci.* **18**, 648–657 (1998).
39. Badio, B. & Daly, J. W. Epibatidine, a potent analgetic and nicotinic agonist. *Mol. Pharmacol.* **45**, 563–569 (1994).
40. Groebe, D. R. & Abramson, S. N. Lophotoxin is a slow binding irreversible inhibitor of nicotinic acetylcholine receptors. *J. Biol. Chem.* **270**, 281–286 (1995).
41. Edelstein, S. J. & Bardsley, W. G. Contributions of individual molecular species to the Hill coefficient for ligand binding by an oligomeric protein. *J. Mol. Biol.* **267**, 10–16 (1997).
42. Zwart, R. & Vijverberg, H. P. Potentiation and inhibition of neuronal nicotinic receptors by atropine: competitive and noncompetitive effects. *Mol. Pharmacol.* **52**, 886–895 (1997).
43. Verbitsky, M., Rothlin, C. V., Katz, E. & Belen Elgoyhen, A. Mixed nicotinic–muscarinic properties of the alpha9 nicotinic cholinergic receptor. *Neuropharmacology* **39**, 2515–2524 (2000).
44. Whatey, J. C., Nass, M. M. & Lester, H. A. Numerical reconstruction of the quantal event at nicotinic synapses. *Biophys. J.* **27**, 145–164 (1979).
45. Land, B. R., Salpeter, E. E. & Salpeter, M. M. Kinetic parameters for acetylcholine interaction in intact neuromuscular junction. *Proc. Natl Acad. Sci. USA* **78**, 7200–7204 (1981).
46. Katz, B. & Miledi, R. The binding of acetylcholine to receptors and its removal from the synaptic cleft. *J. Physiol.* **231**, 549–574 (1973).
47. Kuffler, S. W. & Yoshikama, D. The number of transmitter molecules in a quantum: an estimate from iontophoretic application of acetylcholine at the neuromuscular synapse. *J. Physiol.* **1**, 465–482 (1975).
48. Syed, N. I., Bulloch, A. G. & Lukowiak, K. *In vitro* reconstruction of the respiratory central pattern generator of the mollusk *Lymnaea*. *Science* **250**, 282–285 (1990).
49. Van Minnen, J., Van De Haar, C., Raap, A. K. & Vreugdenhil, E. Localization of ovulation hormone-like neuropeptide in the central nervous system of the snail *Lymnaea stagnalis* by means of immunocytochemistry and *in situ* hybridization. *Cell Tissue Res.* **251**, 477–484 (1988).
50. Slot, J. W., Geuze, H. J. & Weerkamp, A. J. Localization of macromolecular components by application of the immunogold technique on cryosectioned bacteria. *Methods Microbiol.* **20**, 211–236 (1988).

Supplementary Information is available on Nature's World-Wide Web site (<http://www.nature.com>) or as paper copy from the London editorial office of *Nature*.

Acknowledgements

We thank S. N. Abramson for bipinnatin-B; E. R. Van Kesteren and Broers-Vendrig for immunocytochemistry; and F. v. Huizen for suggestions and reagents for the pharmacological experiments. A.B.S. and K.B. were supported by a grant of the Organization for Applied Research (STW). N.I.S. is an Alberta Heritage Foundation for Medical Research senior scholar and was supported by CIHR and NSERC (Canada), and by the Dutch NWO.

Correspondence and request for materials should be addressed to A.B.S. (e-mail: absmit@bio.vu.nl). AChBP Genbank accession number: AF364899.